MR. JOHN ENGLISH (Orcid ID : 0000-0003-4937-6992)

Article type : Research article

Rob Marrs

Article Type:

Research article

Title:

The effect of urban temperature gradients on grassland microclimate amelioration in Los Angeles, USA

Running title:

Microclimate amelioration in urban gradients

Authors:

John English[1*], Alexandra J. Wright[1]

[1*]California State University Los Angeles, Department of Biological Sciences, 5151 State University Dr, Los Angeles CA 90032. Phone: 305-989-0226

This is the author manuscript accepted for publication and has undergone full peer review but has not been through the copyediting, typesetting, pagination and proofreading process, which may lead to differences between this version and the Version of Record. Please cite this article as doi: 10.1111/AVSC.12556

Corresponding author:
John English, Biological Sciences, CSU Los Angeles, Los Angeles, CA, USA
Email- jenglis2@calstatela.edu

Funding information: This work was supported by a NOAA CIMEC Education Outreach Grant (ID #231688) as well as startup funds provided by California State University Los Angeles awarded to Alexandra Wright.

Abstract:

Aim

Microclimate amelioration between neighboring plants may be more common in environments with greater abiotic stress. This pattern has been shown in deserts, alpine systems, and forests, but has not been explored along urban severity gradients. In this study we hypothesized that strong temperature gradients in the greater Los Angeles area might be driving changes in microclimate amelioration in annual grasslands.

Location

Twenty-seven sites along a 100km latitudinal, 72km longitudinal urban gradient across the greater Los Angeles area in California, USA.

Methods

We measured macro- and microclimate variables during the 2019 growing season. We took measurements of temperature, humidity, and vapor pressure deficit (VPD) at the site level as well as under grass canopies.

Results

We found strong cooling effects of the vegetation during the day and warming effects from vegetation at night. We found that these effects were strongest on the hottest/driest days and at the hottest (and often most urban) sites.

*Conclusion*s

Our microclimate amelioration data suggest that positive interactions might become stronger along urban temperature gradients and may be determining plant interactions in these areas in a way that was not previously considered.

Keywords: temperature, humidity, vapor pressure deficit, facilitation, stress gradient hypothesis, urban ecology, heat islands, California grasslands

Introduction:

The stress gradient hypothesis states that as abiotic or biotic stresses become more harsh, the effect of positive interactions between neighbors may increase (Bertness & Callaway 1994). These positive facilitative interactions can vary widely in mechanism. Previous work has shown that some plant species construct novel environments (e.g. niche construction via structural support or shade), increase habitat complexity (heterogeneity), increase service sharing (e.g. pollinator visitation), provide greater access to resources (e.g. nitrogen enrichment from legumes), and provide abiotic stress amelioration (e.g. soil warning in cold or shading in hot conditions) (Cavieres *et al.* 2007; Barbosa *et al.* 2009; McIntire & Fajardo 2014). When abiotic or biotic stresses are limiting productivity, the alleviation of these conditions by facilitation may drive plant-plant interactions more strongly than competition for limiting resources.

One type of positive interaction between plants is amelioration of stressful microclimate conditions (e.g. near-leaf climatic conditions, Brooker *et al.* 2008). Microclimate amelioration is a broad concept that can include: mitigation of solar irradiance that is causing photoinhibition (Kothari *et al.* 2018), reduction of microclimate VPD (Wright *et al.* 2015), and retention of soil water (Caldeira *et al.* 2001). Simply put, microclimate amelioration is the difference between the local climatic conditions organisms are experiencing and their macroclimate, or the "free air" conditions of well-mixed air in nearby open areas (De Frenne *et al.* 2019). This buffering effect of vegetation cover has been shown to have many biological impacts. In arid conditions, plants can increase the water potential of neighbors via physical (e.g. shading) and biological (e.g. evaporative cooling) mechanisms (Wright *et al.* 2015). Through evapotranspiration, plants release water vapor, resulting in a lower near-leaf vapor pressure deficit (VPD; i.e. cooler and more humid environment) for themselves (Meinzer 1993) and neighboring individuals (Wright et al. 2014). This is important for plant performance as VPD drives the evaporative pull of the surrounding air on the leaf (Wever *et al.* 2002). If plant individuals are exposed to high VPD conditions for an extended period of time, this increased evaporative pull can cause severe water stress, embolism, and increased mortality (Kavanagh & Zaerr 1997; Jacobsen *et al.* 2007).

In forests, past work has shown that vegetation can act as a thermal insulator against warming land temperatures, likely mitigating the negative impacts of climate change on biodiversity and functioning (De Frenne *et al.* 2019). Microclimates have also been shown to control the rate of range shifts due to climate change-induced macroclimate warming (Zellweger *et al.* 2020). Vegetation driven microclimate amelioration has been shown to be biologically relevant even over short temporal and small spatial scales. Previous research in annual grasslands has shown that the relative effect of microclimate amelioration can vary on timescales as short as day-to-day. Wright et al. (2015) showed that on relatively cool and humid days, the effect of microclimate amelioration was practically non-existent. This meant that plant interactions were structured entirely by competition for soil water. Conversely, these authors showed that on hotter and drier days, the effect of microclimate amelioration was much stronger and outweighed the impact of competition for soil water.

While vegetation driven microclimate amelioration has been examined extensively in the past in deserts and alpine ecosystems (Brooker *et al.* 2008), no study to date has assessed this type of microclimate amelioration in urban ecosystems or along urban temperature gradients. This is significant given that the stress gradient hypothesis states that microclimate amelioration via vegetation buffering may increase as abiotic or biotic stresses become more harsh (Wright *et al.* 2014; De Frenne *et al.* 2019). Cities create thermal patches that are significantly warmer than surrounding rural areas. These so-called "heat islands" (Taha 2017) are caused by high levels of impervious surfaces that retain thermal energy, higher rates of greenhouse gas emissions, and reduced airflow due to large buildings (McPherson & Simpson 2003; McPherson *et al.* 2011; Stewart & Oke 2012).

In cities like Los Angeles, CA, USA, these urban temperature gradients are further exacerbated by elevational and coastal temperature gradients. In fact, between coastal areas of Los Angeles county where heat islands dissipate and inland areas where heat islands are quite strong, there is an average temperature difference of 5-7°C (Taha 2017). Southern California, where Los Angeles is located, serves as a valuable study system given the ubiquity of grasslands across these many environmental gradients (Sandel & Dangremond 2012; Valliere *et al.* 2017). This allows us to examine microclimate amelioration in the widely used model system, but across an urban gradient. We thus posit that there should be a gradient of increasing microclimate amelioration effects in annual grasslands along temperature gradients in and around Los Angeles County.

To investigate the change in microclimate effects in urban environments, we will test the following two hypotheses: **(H1)** Microclimate amelioration is stronger in hotter areas of Los Angeles: this includes more urban areas as well as areas further from the coast, **(H2)** Microclimate amelioration is stronger on hotter and drier days.

Methods:

<u>Study Area</u>: Our study area encompassed the greater Los Angeles area, CA, USA, covering over 10,000 km^2 ranging from the San Gabriel mountain range to the north to the Santa Ana mountain range to the south, and the Los Angeles county barrier to the east (Figure 1a). The Southern California region, composed of six counties (i.e. Imperial, Los Angeles, Orange, Riverside, San Bernardino, and Ventura), is located within a Mediterranean climate. Grasslands in this area are dominated by exotic, mostly annual, grass species from the Mediterranean region that have established likely due to a history of cattle grazing and changing climate (HilleRisLambers *et al.* 2010; Sandel & Dangremond 2012). This climate is associated with wet winters with cool temperatures and dry summers with high temperatures (Gómez *et al.* 2004). Precipitation during the growing season (November, December, January, February, March, and April) from 1969-2018 averaged 614.68 mm and ranged between 167.64 mm to 1513.84 mm (Figure 2, PRISM Climate Group, Oregon State University). Mean surface temperature over the same period of time was 6.9°C and ranged from 4.6°C to 8.4°C. Precipitation during the growing season in the year of our study (2019) totaled 918.95 mm. Mean surface temperature was 8.3°C and ranged from 2.2°C to 12.9°C. Specifically, total precipitation during our data collection (April 8th-22nd, 2019) across all of our sites averaged 4.9 mm and ranged between 0 mm to 12.3 mm (PRISM Climate Group, Oregon State University). Mean surface temperatures during our data collection ranged from 13.9°C to 17.8°C.

<u>Site Selection</u>: Potential field locations were identified using ArcMap (Version 10.5) where we selected within a range of a 5-30% slope, ≤ 1,200 m elevation, ≥ 1,400 m^2 size, and south-facing aspect. In order to ensure sampling across urbanization levels without confounding urbanization with latitude or longitude, we identified 15 quadrants throughout the greater Los Angeles region (Figure 1b). Seven of these were urban, four were suburban, and four were rural. We then chose nine quadrants from this total of 15 identified: three quadrants randomly chosen from the four available were in rural areas, three randomly chosen from four were in suburban areas, and three randomly chosen from seven were in urban areas. These were large subsections of the city

wherein we could focus our efforts to delineate candidate green spaces to use as our sampling sites.

Within each of these quadrants, all green spaces that were larger than 100 m^2, and met the above physical criteria, were identified and delineated using ArcGIS. Of these, three local sampling sites were randomly selected from each of our nine quadrants (27 local sampling sites). Sampling sites were then ground-truthed to confirm they were unmanaged & unmaintained grasslands. If a site was being actively managed by the community (e.g. mowing or native species planting), it was removed from the dataset and replaced with a newly randomly selected site. This resulted in a total of 27 locations (Figure 1a). At each of these locations three 1 m x 1 m quadrats were randomly selected as our sampling area for our vegetation surveys (81 quadrats total, Figure 1b). Additionally, we created a circular buffer with a 2 km radius centered in the geographic middle of our three sampling quadrats and used image classification to determine the surrounding percent impervious surface of each site (area within the buffer). For each site we also measured elevation and distance to nearest coastline as two other stronger drivers of temperature, site humidity, and site VPD along our urban gradient. To determine if there were differences in soil moisture availability, we measured soil moisture (SM150 soil moisture probe, Dynamax Inc., Huston, TX, USA) on the day we conducted our vegetation survey at the four corners of each of our 1m x 1m quadrats. These four measurements per quadrat were averaged for all analyses.

<u>Microclimate Survey</u>: Peak biomass in annual grasslands of Southern California usually happens in mid-April to late-May (Eviner & Firestone 2007). Because we were interested in the role that vegetation plays in microclimate amelioration, we thus recorded temperature and humidity at our sampling area (which we then used to calculate VPD; Walter *et al.* 2005) over a 15-day period from April 8th - 22nd, 2019 (n = 27):

$$VPD = \left(0.6108 \times e^{\frac{17.27 \times Temp}{Temp + 237.3}} - \left(\frac{RH}{100} \times 0.6108 \times e^{\frac{17.27 \times Temp}{Temp + 237.3}}\right)\right) \qquad \text{Eq. 1}$$

Data were collected at 5-minute intervals using iButton dataloggers (DS1922L Thermochron, Maxim Integrated, San Jose, California) attached to a white 1 m PVC pipe that was stuck approximately 30 cm into the ground (iButtons were thus ~10 cm from the ground). In order to see the effect of the plant canopy on these measurements (so-called microclimate amelioration effects), we installed a pair of dataloggers at each of our 27 sites for a total of 54 individual dataloggers (Figure 1c). The first datalogger of the pair was placed within one randomly chosen quadrat at each site (27 total in the experiment) and installed below the grass canopy at 10 cm above the soil to determine vegetation induced microclimate conditions. The second datalogger was placed within five meters, in a bare patch of soil and located the same distance from the ground and with the same aspect to determine macroclimate conditions (i.e. ambient site conditions, Figure 1c). Dataloggers were wrapped in No. 14 fiberglass screen mesh that provides over 75% of UV protection. This was done to ensure proper airflow and reduce direct irradiation off the metal surface of the datalogger (thus increasing surface temperatures above ambient conditions). After dataloggers had been wrapped in mesh they were secured to white PVC with cable ties. Once collected, microclimate data were categorized into "Day" and "Night" hours to examine site effects for day and night separately. "Day" hours spanned from sunrise to sunset, whereas "night" hours were from sunset and sunrise. Sunrise and sunset were based on times from the first day of our study period (April 8th, 2019).

Vegetation Survey: In order to ensure that differences in community composition along this urban gradient were not driving any observed microclimate effects, we conducted vegetation surveys at each of our sites (Appendix S1). During April 2019, we determined species identity and abundance at each of 81 quadrats at our 27 sites. In addition to our microclimate sampling quadrat, we sampled two additional 1 m x 1 m sampling quadrats to measure percent cover of all species (Figure 1a). We selected these additional quadrats to ensure that we were not missing rare species that may play an important role in this ecosystem. For plants that we could not identify to the species-level we grouped them as one genera. In order to estimate abundance, we visually determined percent cover of each individual species in each quadrat. We also measured percent cover of bare soil (i.e. where no vegetation was present) to determine vegetation density in each quadrat. Given that above average spring rainfall extends the flowering season for California grassland species (Figure 2, Harrison 1999), we were able to sample early-flowering species (e.g. *Phacelia campanularia*, Boraginaceae) to late-flowering species (e.g. *Centaurea melitensis*, Asteraceae).

At each of the three quadrats per site we used our species abundance and evenness data to determine site diversity using the Shannon diversity index (Shannon & Weaver 1964). We also assessed multidimensional scaling (NMDS) axes that summarized community composition from our vegetation survey with RStudio statistical computing software version 2.2-2 (RStudio Team

2020), nlme (v3.1-148; Jose Pinheiro *et al.* 2020), lme4 (v1.1-23; Bates *et al.* 2015), and AICcmodavg (v2.3-0; Mazerolle 2020) packages. Ordination via NMDS was used to determine patterns in community composition and was conducted using the vegan package (Appendix S2; v2.5-6; Oksanen *et al.* 2019; Orme 2012). We found that our first three axes returned a stress value of 0.152. Given that this provides a relatively good fit (Kwak & Peterson 2007), we limited our subsequent analyses to the first three axes.

Data Analysis:

Macroclimate gradients: biogeographical factors

To address the first part of hypothesis one (whether urbanization and coastal effects drive changes in macroclimate factors), we ran multiple linear mixed-effects models using the lme4 package (Appendix S3a; v1.1-23; Bates *et al.* 2015). We used a dataset wherein macroclimate data (temperature, humidity, and VPD) were averaged across the study period at each site (i.e. we computed the mean over the entire study period for a given plot location). We used this dataset as we were concerned with how some areas of the city are hotter than other areas of the city on average, rather than how they vary on a daily basis. We included quadrant as a random effect to account for the blocking effect of sampling sites clustering within their respective quadrants (Figure 1a). Surrounding percent impervious surface, elevation, and distance from nearest coast were all individually included as continuous fixed effects. Average site temperature (averaged over the entire study period), humidity, VPD, and average site soil moisture were included as continuous response variables (nlme package v.3.1-148; Jose Pinheiro *et al.* 2020).

Microclimate gradients: differences between sites

To address the second part of our first hypothesis, that microclimate amelioration is stronger in hotter areas of the city, we conducted a linear mixed-effects model selection to determine which factors best explained microclimate amelioration. We measured microclimate amelioration as:

$$Microclimate\ Amelioration = Macro_i - Micro_i \quad \text{Eq. 2}$$

Where macro is the temperature measured by the iButton in a nearby bareground area, micro is the temperature measured by the iButton under the vegetation, and *i* represents the site (27 total, Figure 1c). For this model selection we used a dataset wherein microclimate amelioration data (temperature, humidity, and VPD) were averaged across the study period at each site (i.e. we computed the mean over the entire study period for a given plot location), because we were interested in the average site effects at each of our study locations for this first hypothesis (not variation from one day to the next). Our model structure had microclimate amelioration (Eq. 2) as our response variable and permutations of macroclimate temperature, elevation, distance to coast, percent impervious surface, Shannon diversity, percent bare ground, and NMDS axes 1-3 as our independent variables (Appendix S3b). We included quadrant as a random effect given the spatial blocking in our sampling design (sites within the same quadrant may be more similar to one another than to other sites within the dataset). Based on the *a priori* design of the experiment, we necessarily included a random effect for quadrant and a fixed effect for macroclimate temperature in all candidate models; Appendix S3c). We calculated R^2 values for each model using the sjstats package (v0.18.0; Ludecke 2020). We also conducted a multivariate correlation matrix (Table 3) to determine if any of these factors were collinear. We found that some factors crossed the 0.5 threshold (our strongest was a negative 0.519 correlation) where collinearity could be determined as high (Dormann *et al.* 2013). To confirm factors were still within acceptable levels of correlation, we determined the variance inflation factor (VIF) using the caret package (v.6.0-86; Kuhn 2020) for all factors and found relatively low correlations with the highest correlation being Shannon index with a score of 3.03. We then used our best fit model and report on the Type I ANOVA results for all main effects associated with this model using the lmerTest package (v.3.1-2; Kuznetsova *et al.* 2017).

Microclimate gradients: differences between days

In order to address our second hypothesis, that microclimate amelioration should be stronger on hotter and drier days, we used a dataset wherein microclimate data were separated into daily measurements at each site (daily measurements per plot) and averaged over each 24-hour period. Our model structure for these analyses differed slightly from the structure for our site averages (Appendix S3d). We retained individual macroclimate predictors (e.g. macro-temperature, macro-humidity, and macro-VPD) and their effects on each individual aspect of microclimate amelioration (micro-temperature, micro-humidity, and micro-VPD respectively, Eq. 2) given that these were measured daily. We included sampling site nested in quadrant as a random effect given that each sampling site can only occur in its respective quadrant. Additionally, since all sampling sites were surveyed at every date, we included date as a crossed random effect in our model structure. We report on the Type I ANOVA results for these models using the lmerTest package (v.3.1-2; Kuznetsova *et al.* 2017). Using this model structure, we then ran the same analyses using our "day" and "night" datasets to see if there were differences during the warmest and coolest parts of the day.

Results

Macroclimate gradients: biogeographic factors

In line with hypothesis one, we found that percent impervious surface had a positive effect on average site temperature but had no effect on humidity or VPD (Table 1, Figure 2a). Additionally, we found that elevation had a negative effect on temperature but did not have an effect on humidity or VPD (Table 1, Figure 2b). Increasing distance from nearest coast did not have an effect on any of our abiotic variables (Table 1). Due to the nature of urban development in Los Angeles, our rural locations were at higher elevations than our suburban and urban locations (Figure 2c). Site average soil moisture did not vary as a function of percent development ($F_{1, 15} = 1.91$, $p = 0.19$), elevation ($F_{1, 15} = 1.25$, $p = 0.28$), or distance to coast ($F_{1, 15} = 0.16$, $p = 0.69$).

Microclimate gradients: differences between sites

We found that the best-fit model for site-level temperature amelioration included average site temperature and NMDS Axis 2 (Table 2). Analyzing this model using the linear mixed effects model framework showed that macroclimate temperature had a positive effect on the strength of microclimate temperature amelioration ($F_{1,16} = 4.32$, $p = 0.054$; Figure 3) while NMDS Axis 2 had no effect on microclimate temperature amelioration ($F_{1,16} = 1.46$, $p = 0.24$). We decided to maintain this overall model structure for all microclimate amelioration analyses to better compare the model effects on all three aspects of microclimate amelioration (temperature, humidity, and VPD). There were no other significant effects of macro-humidity or macro-VPD on average microclimate amelioration between sites.

Microclimate gradients: differences between days

We found that as daily site temperatures increased, the temperature under the plant canopy warmed less than ambient conditions ($F_{1, 38.5} = 71.49$, $p < 0.001$; Figure 4a). Additionally, we found that as daily humidity decreased at sites, the humidity under the plant canopy retained more moisture ($F_{1, 128.6} = 170.65$, $p < 0.001$; Figure 4b). Measures of VPD showed that on days where there was increasingly high VPD (hot and dry days), the plant canopy had an increasingly strong effect on VPD reduction (it was cooler and more humid under the plants ($F_{1, 196.3} = 155.85$, $p < 0.001$ Figure 4c).

We also found strong day / night differences in temperature, humidity, and VPD (Figure 4). When examined during daytime hours (daily sunrise to sunset), the plant canopy had a strong cooling effect on temperature ($F_{1, 29.5} = 84.42$, $p < 0.001$; Figure 4d), approached significance for reducing humidity ($F_{1, 25.7} = 3.22$, $p = 0.084$; Figure 4e), and a moderating effect on daytime VPD ($F_{1, 141.9} = 153.88$; Figure 4f). In general, nighttime effects showed the opposite: as temperatures decreased, the air under the plant canopy was warmer than ambient temperatures ($F_{1, 21.1} = 73.61$, $p < 0.001$; Figure 4g), while humidity levels were lower ($F_{1, 40.2} = 192.13$, $p < 0.001$; Figure 4h), and VPD was lower ($F_{1, 48.7} = 132.89$, $p < 0.001$; Figure 4i).

Discussion

We found evidence for variation in the strength of microclimate amelioration along an urban to rural gradient in the greater Los Angeles county area. We found support for our hypothesis that during the day, more densely developed sites were hotter and these hotter sites experienced progressively stronger microclimate amelioration effects. For sites that had an average macroclimate (i.e. bare ground, soil-level) temperature of 14°C during our April study period (e.g. Briar Summit), there was an average temperature reduction of 2°C in their microclimate (i.e. under the vegetation) across the entire study period. Conversely, sites that had cooler average temperatures (in more rural areas) experienced weaker microclimate amelioration effects. Sites that had an average temperature of 7°C (e.g. Musch Meadows) had no average change in under canopy microclimate. While our data set is limited (due to number of sites and days sampled), plant individuals in locations across this urban temperature gradient appear to experience different microsite conditions, at least for part of their growing season.

These data also support our hypothesis that hotter days result in stronger microclimate amelioration. All three measures of microclimate (i.e. temperature, humidity, and VPD) responded differently in under-canopy measurements. Higher temperatures were cooled during the day while cooler temperatures were warmed during the night. These effects were particularly noticeable on hot, dry days where we saw a strong buffering effect of vegetation. When we looked at vegetation effects in terms of humidity, we found there was only a weak effect of vegetation on humidity during daylight hours. However, when *nighttime* macroclimate humidity was low, under-canopy humidity was increased. During both day and night, high VPD was decreased under the plant canopy.

These findings are consistent with previous research showing that vegetation driven microclimate amelioration can increase during periods of warming and drought (Wright *et al.* 2015; De Frenne *et al.* 2019; Zellweger *et al.* 2020). In a global meta-analysis, De Frenne et al. (2019) demonstrated that maximum and mean temperatures were consistently cooler and minimum temperatures were consistently warmer within forests compared to free-air temperatures. During one season, we report similar trends in short-stature annual grasslands. We report that not only was microclimate amelioration generally stronger at hotter sites, but regardless of location, there were differences in microclimate depending on daily environmental severity (temperature and humidity). The stress-gradient hypothesis not only appears to be functioning across a physical gradient, but a temporal environmental gradient experienced by all sites as well.

The alleviation of these abiotic conditions is particularly important in Southern California's arid Mediterranean climate. Evapotranspiration is higher from surfaces receiving more solar energy and from more exposed locations where wind speeds are higher (Bramer *et al.* 2018). Lower irradiation often results in plant individuals that are less water stressed and photoinhibited under the plant canopy, potentially increasing survival rates (Baquedano & Castillo 2006). Increasing microclimate humidity also has beneficial effects, given that stomatal conductance is directly linked to humidity near the leaf (Wever *et al.* 2002).

Further, these shifts in microclimate conditions may be particularly important in the context of climate change. The growing season in California annual grasslands begins in November and ends in May, when average daytime VPD ranges from around 0 – 2 kPa (Ryu *et al.* 2008). As aridity is expected to increase in the Southwest in the future (Cook *et al.* 2015), the ability to maintain VPD values below 2 kPa may become more important to mitigate the regional effects of warming and drought. In fact, previous research in other grasslands and croplands has shown that reductions in vapor pressure deficit from 2 kPa to 1 kPa can cause significant increases in overall herbaceous plant growth (Ray *et al.* 2002; Wright *et al.* 2014).

We also found evidence for nighttime buffering of lower temperatures. Unlike daytime heat mitigation which may be partially driven by evapotranspiration (Wright *et al.* 2015), this nighttime buffering is possibly driven by two separate mechanisms. The first is a physical mechanism: vegetation may insulate and capture heat that is either captured during daylight hours or re-radiated from the soil surface at night. In fact, during the night in open (i.e. nonvegetated) areas, ground temperatures can even be cooler than air temperatures above the boundary layer (Bramer *et al.* 2018). Past work has shown that vegetation can effectively buffer against negative effects of wind and provide thermal amelioration in forest and alpine systems (Callaway *et al.* 2002; Arroyo *et al.* 2003; Cavieres *et al.* 2006; De Frenne *et al.* 2019). Further support for this comes from studies showing that microstructures such as stumps and branches reduce wind velocities, consequently increasing plot temperatures (Proe *et al.* 2001). There may be higher temperatures in our nighttime plots via a physical blocking of wind resulting in higher retention of thermal energy.

The second mechanism driving nighttime microclimate amelioration may be nighttime transpiration, the process of water movement through a plant ending with its evaporation from the stem or leaf surface. In a metanalysis by Dawson et al. (2007), the authors showed that many plant species perform nighttime transpiration, sometimes accounting for a significant fraction of total daily water use. This was particularly true in drought-prone ecosystems where nighttime VPD exceeded ~0.7 kPa (Dawson *et al.* 2007). While we did not directly measure stomatal conductance or transpiration, our data show a similar trend. We found that as nighttime VPD increased, under canopy humidity increased (Appendix S4). In our plots that had nighttime VPD values above 0.7 kPa, there was an average increase in humidity by 4.6% from ambient levels. Future studies should look more directly into transpiration of these annual grasslands as the water budgets in these systems may be influenced by nighttime transpiration effects (Dawson *et al.* 2007).

Conclusion

Our data support the hypothesis that vegetation driven microclimate amelioration is stronger in hotter, more stressful area of an urban ecosystem. These data also support the theory that there are temporal shifts in biotic interactions that may occur from day to day between the same neighbors (Wright *et al.* 2014; De Frenne *et al.* 2019). Not only did we find hotter sites had higher instances of microclimate amelioration, but that amelioration had daily variation. Given the magnitude of microclimate amelioration seen in our data, future work should focus on whether there is a shift from competitive to facilitative species interactions across this gradient. Should there be significant influences on species interactions due to microclimate effects, it may better inform how we can manage plant communities in developed areas.

Author contributions:

A. J. W. conceived the experiment and provided partial funding. J. E. and A. J. W. established the experimental design. J. E. collected the data, analyzed the data, and wrote the first draft of the manuscript. Both authors contributed extensively to the final draft.

Data accessibility:

The data that support the findings of this study have been uploaded to Dryad are available upon request from the corresponding author (https://doi.org/10.5061/dryad.05qfttf1x).

Online appendices:

Appendix S1. List of all identified plant organisms.

Appendix S2. NMDS of different urbanization categories

Appendix S3. Model formulas for conducted analyses.

Appendix S4. Effect of nighttime VPD on under canopy humidity.

References:

Arroyo, M.T.K., Cavieres, L.A. & Peñaloza, A. (2003). Positive associations between the cushion plant Azorella monantha (Apiaceae) and alpine plant species in the Chilean Patagonian Andes. *Plant Ecol.*, 169, 121–129.

Baquedano, F.J. & Castillo, F.J. (2006). Comparative ecophysiological effects of drought on seedlings of the Mediterranean water-saver Pinus halepensis and water-spenders Quercus coccifera and Quercus ilex. *Trees*, 20, 689–700.

Barbosa, P., Hines, J., Kaplan, I., Martinson, H. & Szczepaniec, A. (2009). Associational Resistance and Associational Susceptibility: Having Right or Wrong Neighbors. *Annu. Rev. Ecol. Evol. Syst.*, 40, 1–20.

Bates, D., Machler, M., Bolker, B. & Walker, S. (2015). Fitting Linear Mixed-Effects Models Using lme4. *J. Stat. Softw.*, 67, 1–48.

Bertness, M.D. & Callaway, R.M. (1994). Positive interactions in communities. *Trends Ecol. Evol.*, 9, 187–191.

Bramer, I., Anderson, B.J., Bennie, J., Bladon, A.J., Frenne, P. De, Hemming, D., *et al.* (2018). Methods of monitoring and modelling microclimate in ecological research. *Adv. Biol. Res. (Rennes).*, 101–161.

Brooker, R.W., Maestre, F.T., Callaway, R.M., Lortie, C.L., Cavieres, L.A., Kunstler, G., *et al.* (2008). Facilitation in plant communities: The past, the present, and the future. *J. Ecol.*, 96, 18–34.

Caldeira, M.C., Ryel, R.J., Lawton, J.H. & Pereira, J.S. (2001). Mechanisms of positive biodiversity-production relationships: insights provided by d13C analysis in experimental Mediterranean grassland plots. *Ecol. Lett.*, 439–443.

Callaway, R.M., Brooker, R.W., Choler, P., Kikvidze, Z., Pugnaire, F.I., Newingham, B., *et al.* (2002). Positive interactions among alpine plants increase with stress. *Lett. to Nat.*, 417, 844–848.

Cavieres, L.A., Badano, E.I., Sierra-Almeida, A., Gómez-González, S. & Molina-Montenegro, M.A. (2006). Positive interactions between alpine plant species and the nurse cushion plant Laretia acaulis do not increase with elevation in the Andes of central Chile. *New Phytol.*, 169, 59–69.

Cavieres, L.A., Badano, E.I., Sierra-Almeida, A. & Molina-Montenegro, M.A. (2007). Microclimatic Modifications of Cushion Plants and Their Consequences for Seedling Survival of Native and Non-native Herbaceous Species in the High Andes of Central Chile. *Arctic, Antarct. Alp. Res.*, 39, 229–236.

Cook, B.I., Ault, T.R. & Smerdon, J.E. (2015). Unprecedented 21st century drought risk in the American Southwest and Central Plains, 1–8.

Dawson, T.E., Burgess, S.S.O., Tu, K.P., Oliveira, R.S., Santiago, L.S., Fisher, J.B., *et al.* (2007). Nighttime transpiration in woody plants from contrasting ecosystems. *Tree Physiol.*, 561–575.

Dormann, C.F., Elith, J., Bacher, S., Buchmann, C., Carl, G., Carré, G., *et al.* (2013). Collinearity: A review of methods to deal with it and a simulation study evaluating their performance. *Ecography (Cop.).*, 36, 27–46.

Eviner, V.T. & Firestone, M.K. (2007). Mechanisms Determining Patterns of Nutrient Dynamics. In: *California Grasslands: Ecology and Management* (eds. Stromberg, M.R., Corbin, J.D. & D'Antonio, C.M.). University of California Press, Berkeley and Los Angeles, California, pp. 94–106.

Frenne, P. De, Zellweger, F., Rodríguez-Sanchez, F., Scheffers, B., Hylander, K., Luoto, M., *et al.* (2019). Global buffering of forest understory temperatures. *Nat. Ecol. Evol.*, 3, 744–749.

Gómez, L., Zamora, R., Gómez, J.M., Hódar, J. a & Castro, J. (2004). Applying Plan Facilitation To Forest Restoration In Mediterranean Ecosystems: A Meta-Analysis Of The Shrubs As Nurse Plants. *Ecol. Appl.*, 14, 1118–1138.

HilleRisLambers, J., Yelenik, S.G., Colman, B.P. & Levine, J.M. (2010). California annual grass invaders: the drivers or passengers of change? *J. Ecol.*, 98, 1147–1156.

Jacobsen, A.L., Pratt, R.B., Davis, S.D. & Ewers, F.W. (2007). Cavitation resistance and seasonal hydraulics differ among three arid Californian plant communities, 1599–1609.

Jose Pinheiro, Bates, D., DebRoy, S., Sarkar, D. & R Core Team. (2020). nlme: Linear and Nonlinear Mixed Effects Models. R package version 3.1-148. https://CRAN.R-project.org/package=nlme.

Kavanagh, K.L. & Zaerr, J.B. (1997). Xylem cavitation and loss of hydraulic conductance in western hemlock following planting. *Tree Physiol.*, 17, 59–64.

Kothari, S., Cavender-Bares, J., Bitan, K., Verhoeven, A.S., Wang, R., Montgomery, R.A., *et al.* (2018). Community-wide consequences of variation in photoprotective physiology among prairie plants. *Photosynthetica*, 56, 455–467.

Kuhn, M. (2020). caret: Classification and Regression Training. R package version 6.0-86. https://CRAN.R-project.org/package=caret.

Kuznetsova, A., Brockhoff, P.B. & Christensen, R.H.B. (2017). lmerTest: Tests in Linear Mixed Effects Models. *J. Stat. Softw.*, 82, 1–26. R package version 3.1-2.

Kwak, T.J. & Peterson, J. (2007). Community indices, parameters, and comparisons. In: *Analysis and interpretation of freshwater fisheries data*. American Fisheries Society, Bethesda, Maryland, pp. 677–763.

Ludecke, D. (2020). sjstats: Statistical Functions for Regression Models. R package version 0.18.0. doi: 10.5281/zenodo.1284472. https://CRAN.R-project.org/package=sjstats.

Mazerolle, M.J. (2020). AICcmodavg: Model selection and multimodel inference based on (Q)AIC(c). R package version 2.3-0. https://cran.r-project.org/package=AICcmodavg.

McIntire, E.J.B. & Fajardo, A. (2014). Facilitation as a ubiquitous driver of biodiversity. *New Phytol.*, 403–416.

McPherson, E.G. & Simpson, J.R. (2003). Potential energy saving in buildings by an urban tree planting programme in California, 3, 73–86.

McPherson, E.G., Simpson, J.R., Xiao, Q. & Wu, C. (2011). Million trees Los Angeles canopy cover and benefit assessment. *Landsc. Urban Plan.*, 99, 40–50.

Oksanen, J., Blanchet, F.G., Friendly, M., Kindt, R., Legendre, P., McGlinn, D., *et al.* (2019). vegan: Community Ecology Package. R package version 2.5-6. https://CRAN.R-project.org/package=vegan.

Orme, D.L. (2012). betapart : an R package for the study of beta diversity. *Methods Ecol. Evol.*, 3, 808–812.

Proe, M.F., Griffiths, J.H. & Mckay, H.M. (2001). Effect of whole-tree harvesting on microclimate during establishment of second rotation forestry, 110, 141–154.

Ray, J.D., Gesch, R.W., Sinclair, T.R. & Allen, L.H. (2002). The effect of vapor pressure deficit on maize transpiration response to a drying soil, 113–121.

Ryu, Y., Baldocchi, D.D., Ma, S. & Hehn, T. (2008). Interannual variability of evapotranspiration and energy exchange over an annual grassland in California. *J. Geophys. Res.*, 113, 1–16.

Sandel, B. & Dangremond, E.M. (2012). Climate change and the invasion of California by grasses. *Glob. Chang. Biol.*, 18, 277–289.

Stewart, I.D. & Oke, T.R. (2012). Local climate zones for urban temperature studies. *Bull. Am. Meteorol. Soc.*, 93, 1879–1900.

Taha, H. (2017). Characterization of Urban Heat and Exacerbation: Development of a Heat Island Index for California. *Climate*, 5, 59.

Team, Rs. (2020). RStudio. Verstion 2.2-2.

Valliere, J.M., Irvine, I.C., Santiago, L. & Allen, E.B. (2017). High N , dry : Experimental nitrogen deposition exacerbates native shrub loss and nonnative plant invasion during extreme drought. *Glob. Chang. Biol.*, 4333–4345.

Walter, I.A., Allen, R.G., Elliott, R., Itenfisu, D., Brown, P., Jensen, M.E., *et al.* (2005). *The ASCE Standardized Reference Evapotranspiration Equation*. American Society of Civil Engineers.

Wever, L.A., Flanagan, L.B. & Carlson, P.J. (2002). Seasonal and interannual variation in evapotranspiration , energy balance and surface conductance in a northern temperate grassland. *Agric. For. Meteorol.*, 112, 31–49.

Wright, A.J., Schnitzer, S.A. & Reich, P.B. (2014). Living close to your neighbors : the importance of both competition and facilitation in plant communities, 95, 2213–2223.

Wright, A.J., Schnitzer, S.A. & Reich, P.B. (2015). Daily environmental conditions determine the competition-facilitation balance for plant water status. *J. Ecol.*, 103, 648–656.

Zellweger, F., de Frenne, P., Lenoir, J., Vangansbeke, P., Verheyen, K., Bernhardt-Römermann, M., *et al.* (2020). Forest microclimate dynamics drive plant responses to warming. *Science (80-.).*, 368, 772–775.

Tables

Table 1. We used a linear mixed-effects model to assess the effects of percent impervious surfaces (Percent Dev), elevation (m), and distance from coast (km) on average daily temperatures (°C), percent relative humidity, and vapor pressure deficit (kPa). We included quadrant as a random effect given the blocked nature of our sampling design. Site temperature, humidity, and VPD were collected at each site using iButton dataloggers.

Fixed Effect	Random Effect	Site Temperature			Humidity			VPD		
		df	F	P	df	F	P	df	F	P
Percent Dev	Quadrant	1, 17	4.03	0.061*	1, 17	0.22	0.65	1, 17	0.18	0.67
Elevation	Quadrant	1, 17	6.79	0.019*	1, 17	1.09	0.31	1, 17	0.28	0.60
Distance From Coast	Quadrant	1, 17	15.93	0.744	1, 17	2.98	0.10	1, 17	0.0096	0.92

Table 2. Model selection for what factors best fit temperature amelioration. Factors included were macro-temperature (Macrotemp), alpha diversity from our Shannon Diversity index calculation (Alpha), NMDS axes 1-3, and percent bare ground of quadrat (Ground). Quadrant was included as a random effect in each model to account for the blocking effect of sampling sites clustering within their respective quadrants.

Model	K	AICc	Delta_AICc	AICcWt	Cum_Wt	Res_LL	R^2
Macrotemp NMDS2	5	124.41	0.00	0.16	0.16	-55.77	0.266
Macrotemp	4	124.43	0.03	0.15	0.31	-57.31	0.230
Macrotemp Alpha	5	125.40	0.99	0.10	0.41	-56.31	0.220
Macrotemp Alpha NMDS2	6	125.59	1.19	0.09	0.49	-54.70	0.261
Macrotemp NMDS3	5	125.70	1.29	0.08	0.57	-56.42	0.263
Macrotemp NMDS2 NMDS3	6	126.06	1.66	0.07	0.64	-54.93	0.265

Macrotemp NMDS1	5	126.43	2.02	0.06	0.70	-56.79	0.212
Macrotemp NMDS1 NMDS2	6	126.70	2.29	0.05	0.75	-55.25	0.240
Macrotemp Alpha NMDS3	6	126.78	2.37	0.05	0.80	-55.29	0.250
Macrotemp Alpha NMDS2 NMDS3	7	127.32	2.92	0.04	0.83	-53.71	0.244
Macrotemp Alpha NMDS1	6	127.36	2.96	0.04	0.87	-55.58	0.184
Macrotemp Alpha NMDS1 NMDS2	7	127.95	3.54	0.03	0.90	-54.03	0.245
Macrotemp NMDS1 NMDS3	6	127.95	3.54	0.03	0.92	-55.87	0.242
Macrotemp Alpha NMDS1 NMDS3	7	128.86	4.45	0.02	0.94	-54.48	0.209
Macrotemp Ground	5	129.28	4.87	0.01	0.95	-58.14	0.310
Macrotemp NMDS2 Ground	6	129.42	5.01	0.01	0.97	-56.50	0.333
Macrotemp Alpha NMDS1 NMDS2 NMDS3	8	129.80	5.39	0.01	0.98	-52.90	0.227
Macrotemp Alpha Ground	6	130.45	6.04	0.01	0.98	-57.01	0.303
Macrotemp NMDS3 Ground	6	130.60	6.19	0.01	0.99	-57.09	0.326
Macrotemp NMDS1 Ground	6	131.61	7.20	0.00	0.99	-57.59	0.296
Macrotemp Alpha NMDS2 NMDS3 Ground	8	132.75	8.35	0.00	1.00	-54.14	0.325
Macrotemp Alpha NMDS1 NMDS2 Ground	8	133.82	9.42	0.00	1.00	-54.68	0.302
Macrotemp Alpha NMDS1 NMDS3 Ground	8	134.63	10.22	0.00	1.00	-55.08	0.209
Macrotemp Alpha NMDS1 NMDS2 NMDS3 Ground	9	135.79	11.38	0.00	1.00	-53.27	0.318

Table 3. Multivariate correlation matrix for factors used in model selection. Factors included were macro-temperature, alpha diversity (Shannon's index), axis one of our NMDS, axis two of our NMDS, axis three of our NMDS, and percent bare ground.

	MacroTemp	Alpha	NMDS1	NMDS2	NMDS3	Bare Ground
MacroTemp		-0.433	-0.462	-0.030	-0.240	0.041
Alpha	-0.433		0.566	-0.371	0.365	0.086
NMDS1	-0.462	0.566		-0.057	-0.014	0.021
NMDS2	-0.030	-0.371	-0.057		0.295	0.088
NMDS3	-0.240	0.365	-0.014	0.295		0.409
Bare Ground	0.041	0.086	0.021	0.088	0.409	

Figures

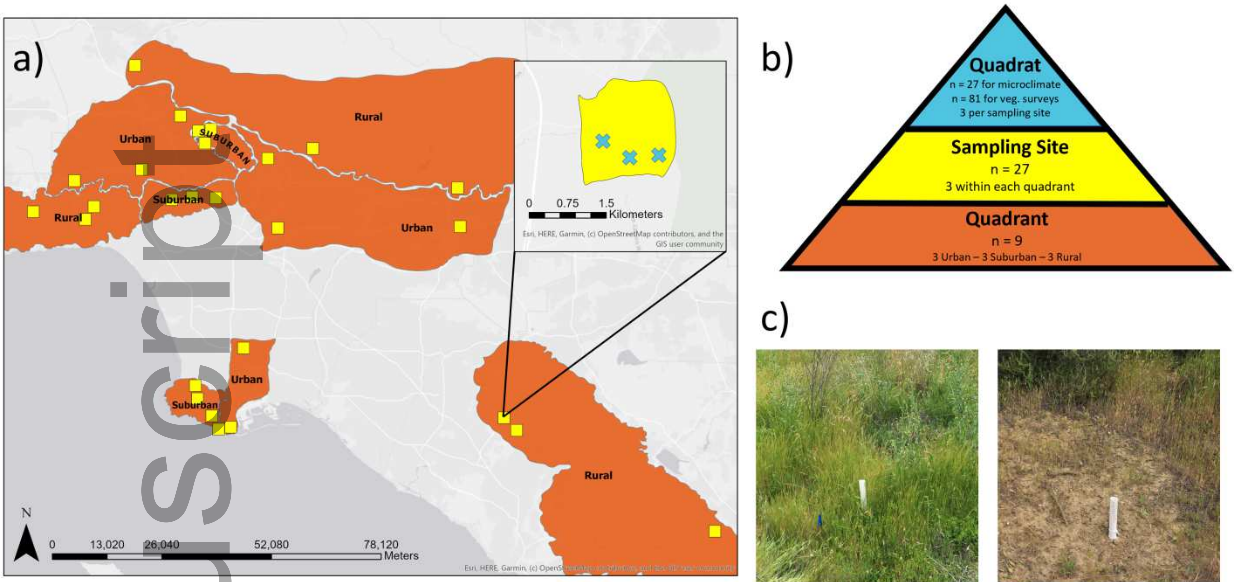

Figure 1. (a) Map of sampling sites across the greater Los Angeles region. Orange polygons depict quadrants, yellow squares depict sampling sites, and blue crosses depict 1 m x 1m quadrats (only one site shown in figure). (b) Conceptual figure of our sampling design with colors corresponding to panel a. (c) Example of a datalogger installed under-canopy for microclimate (left) and example of a datalogger installed in bare ground for macroclimate conditions (right).

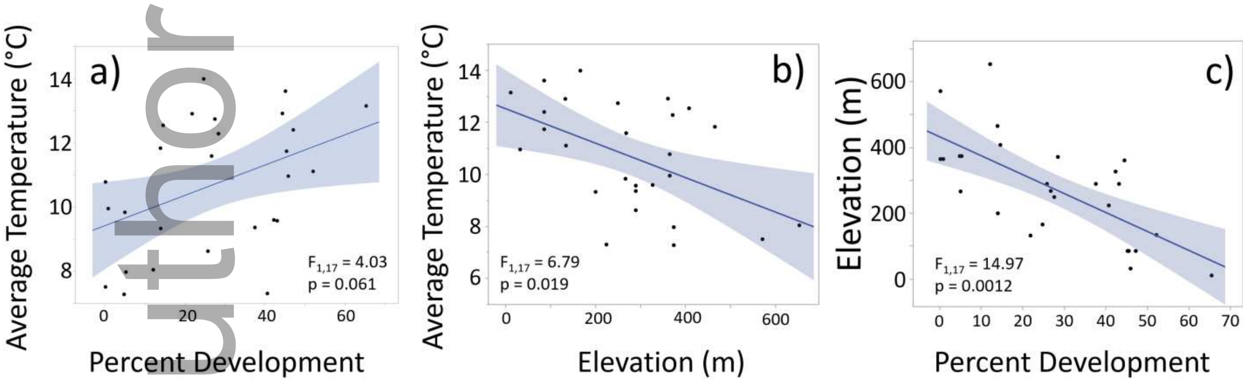

Figure 2. The effects of abiotic factors on macroclimate temperature. We gathered temperature data every 5 minutes from iButton dataloggers over the course of two weeks at each site. We assessed (a) the effect of percent impervious surface (Percent Development) on average temperature at the sites (°C), (b) the effect of elevation on average temperature at the sites, and (c) the correlation between percent impervious surface (Percent Development) and elevation.

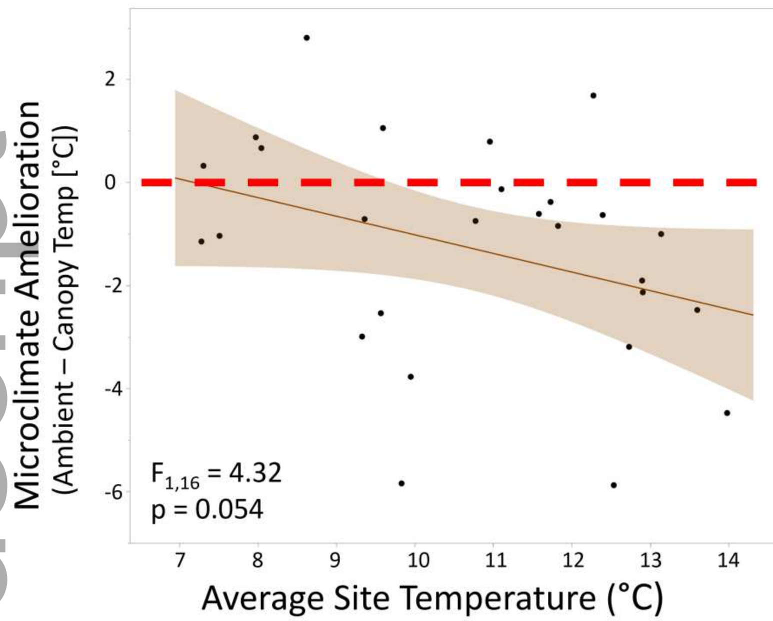

Figure 3. The effect of average site temperature on microclimate amelioration. We gathered temperature data every 5 minutes from iButton dataloggers and averaged these values across the entire two-week period for each site. The dashed line represents no difference between ambient and under-canopy measurements. Points represent a warming (higher than 0) or cooling (lower

than 0) effect of vegetation.

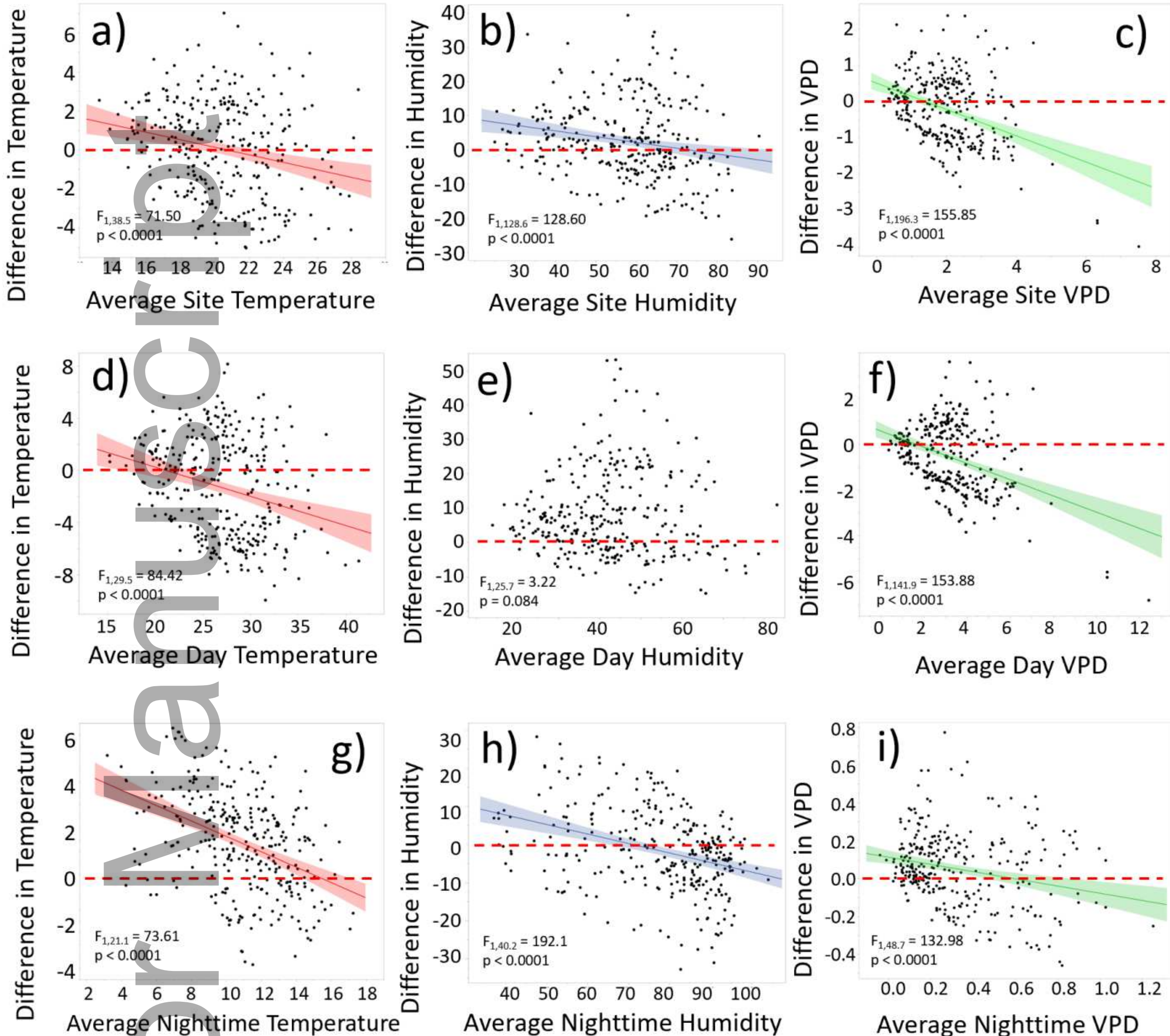

Figure 4. We measured site conditions (x-axes) and microclimate amelioration variables (y-axes) across 24-hour periods (a-c), daylight hours (d-f), and nighttime hours (g-i). Each point represents the average value at that site on that day. Dashed lines represent no difference between ambient and under-canopy measurements. In the case of temperature, points represent a warming (higher than 0) or cooling (lower than 0) effect of vegetation.

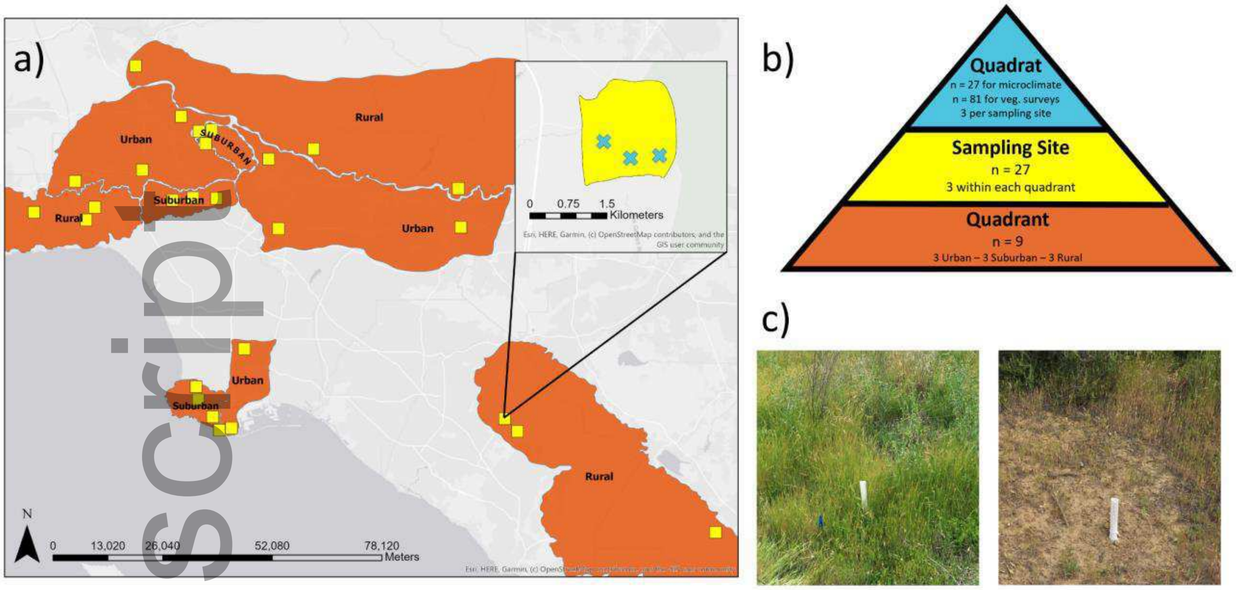

Figure 1. (a) Map of sampling sites across the greater Los Angeles region. Orange polygons depict quadrants, yellow squares depict sampling sites, and blue crosses depict 1 m x 1m quadrats (only one site shown in figure). (b) Conceptual figure of our sampling design with colors corresponding to panel a. (c) Example of a datalogger installed under-canopy for microclimate (left) and example of a datalogger installed in bare ground for macroclimate conditions (right).

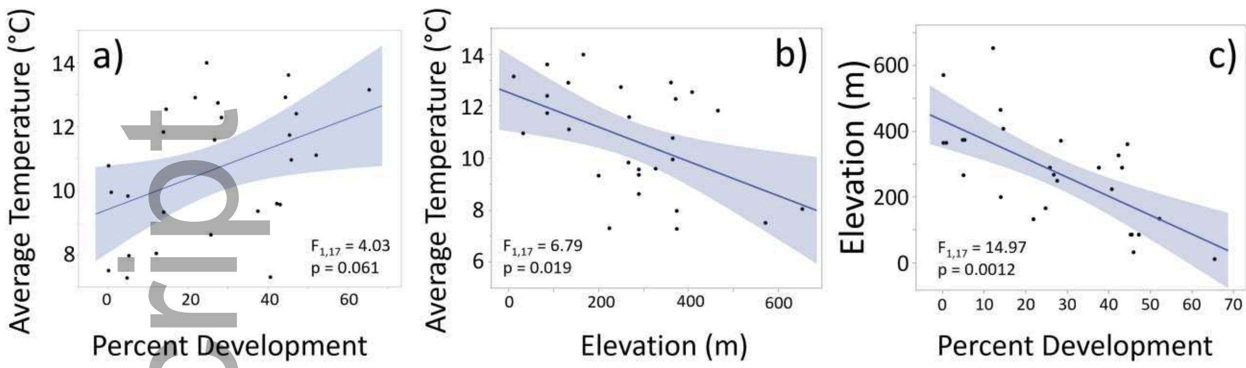

Figure 2. The effects of abiotic factors on macroclimate temperature. We gathered temperature data every 5 minutes from iButton dataloggers over the course of two weeks at each site. We assessed (a) the effect of percent impervious surface (Percent Development) on average temperature at the sites (°C), (b) the effect of elevation on average temperature at the sites, and (c) the correlation between percent impervious surface (Percent Development) and elevation.

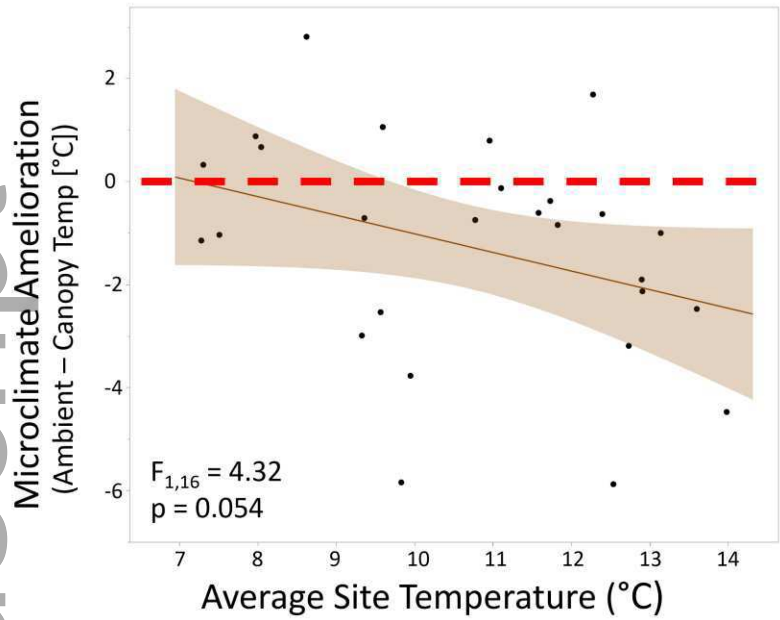

Figure 3. The effect of average site temperature on microclimate amelioration. We gathered temperature data every 5 minutes from iButton dataloggers and averaged these values across the entire two-week period for each site. The dashed line represents no difference between ambient and under-canopy measurements. Points represent a warming (higher than 0) or cooling (lower than 0) effect of vegetation.

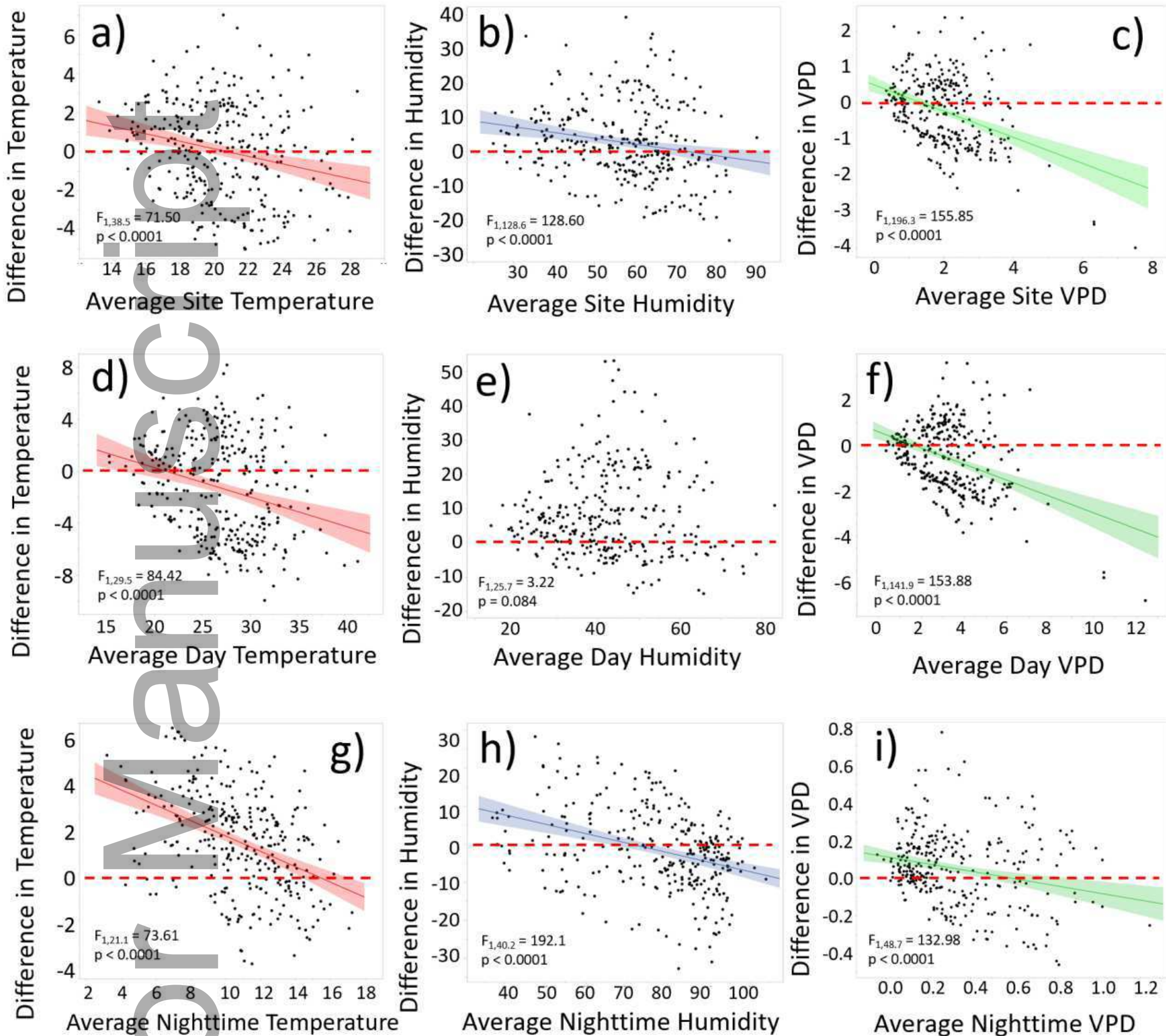

Figure 4. We measured site conditions (x-axes) and microclimate amelioration variables (y-axes) across 24-hour periods (a-c), daylight hours (d-f), and nighttime hours (g-i). Each point represents the average value at that site on that day. Dashed lines represent no difference between ambient and under-canopy measurements. In the case of temperature, points represent a warming (higher than 0) or cooling (lower than 0) effect of vegetation.